Electronic Supplementary Material (ESI) for Physical Chemistry Chemical Physics.

Supporting Information

Metal Borohydride Formation from Aluminium Boride and Metal Hydrides

Kasper T. Møller,[1] Alexander S. Fogh,[1] Mark Paskevicius,[1] Jørgen Skibsted,[1] Torben R. Jensen[1*]

[1]*Interdisciplinary Nanoscience Center (iNANO) and Department of Chemistry, University of Aarhus, DK-8000 Aarhus, Denmark*

*Corresponding Author

Torben R. Jensen, Dr. Scient, Professor

Center for Materials Crystallography

iNANO and Department of Chemistry

Langelandsgade 140

D-8000 Aarhus C

Aarhus University

Denmark

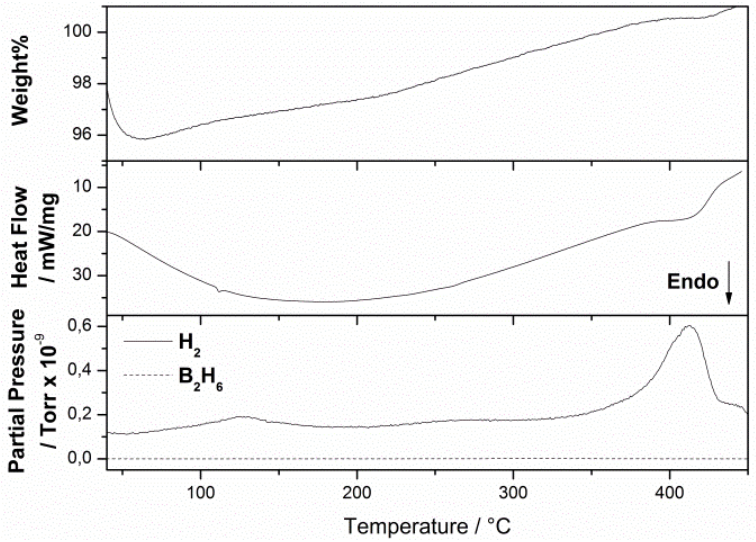

Figure S1. TG-DSC-MS of the sample Li_100bar_12h heated from RT to 450 °C with $\Delta T/\Delta t$ = 5 K/min.

The TG-DSC-MS data for the sample Li_100bar_12h further confirms the formation of $LiBH_4$. An endothermic peak is present at T = 110 °C which is owing to the phase transition from *o*-$LiBH_4$ to *h*-$LiBH_4$.[1,2] At T = 260 °C another endothermic peaks is present which belongs to the melting of $LiBH_4$.[3,4] Finally, a hydrogen release (m/z = 2) is observed in MS together with an endothermic DSC event as the $LiBH_4$ starts to decompose at T ~ 370 °C.[5] Finally, no release of diborane (m/z = 27) is observed.

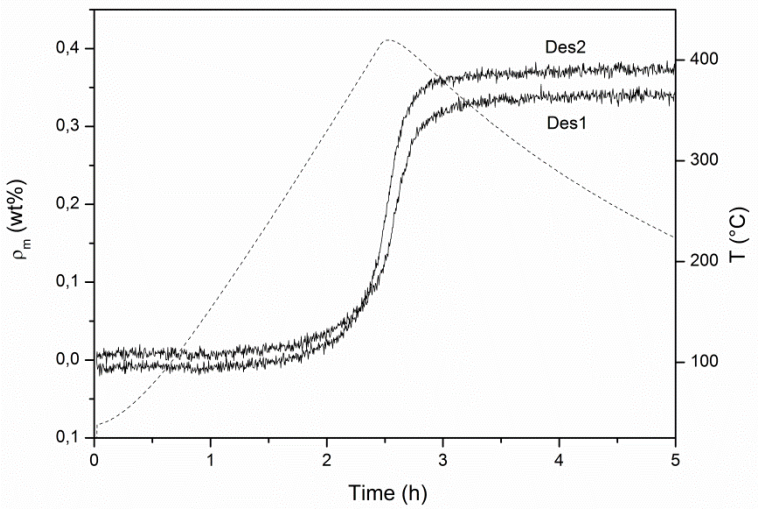

Figure S2. Sieverts' measurement of the sample Li_100bar_12h heated from RT to 450 °C with $\Delta T/\Delta t$ = 3 K/min.

In Sieverts' measurement both the first and second desorption of Li_100bar_12h shows a gas release starting at T ~ 360 °C and the release amounts to 0.36 and 0.40 wt%, respectively. The decomposition temperature is in good agreement with the TG-DSC-MS experiment.

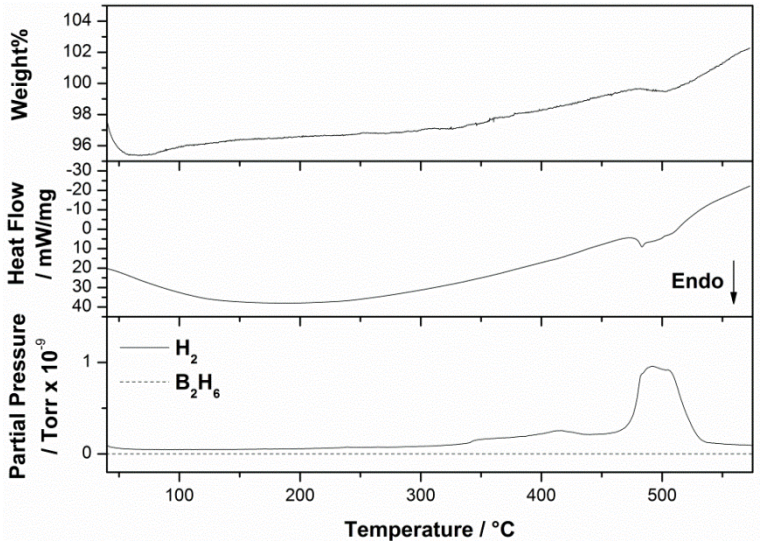

Figure S3. TG-DSC-MS of the sample Na_100bar_12h heated from RT to 575 °C with $\Delta T/\Delta t$ = 5 K/min.

The Na_100bar_12h sample shows an endothermic hydrogen release at T = 485 °C which is 50 °C lower than the reported decomposition temperature of neat $NaBH_4$ at T = 535 °C.[6] This may indicate a destabilisation of $NaBH_4$ by Al. Additionally, a small hydrogen release is observed at T ~ 340 °C which probably owes to an excess of NaH.

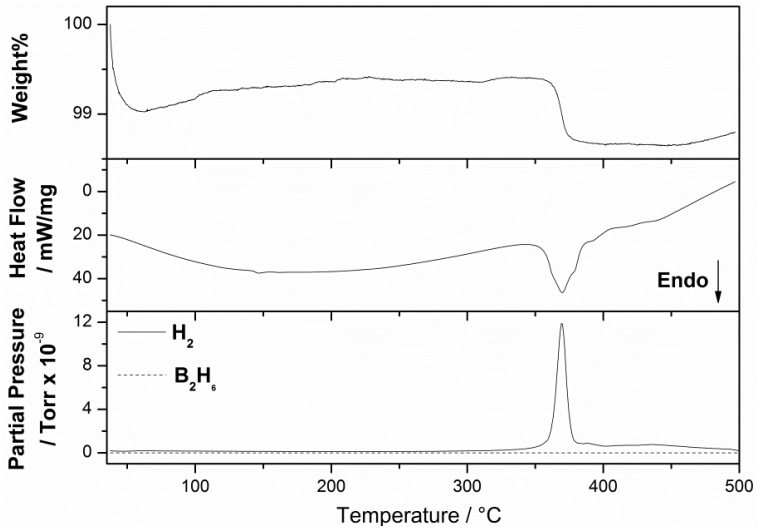

Figure S4. TG-DSC-MS of the sample Ca_100bar_12h heated from RT to 500 °C with $\Delta T/\Delta t$ = 5 K/min.

The phase transition from α- to β-$Ca(BH_4)_2$ is observed as an endothermic peak at T = 145 °C.[7–9] Additionally, an endothermic hydrogen release is observed with a peak at T = 345 °C which is 22 °C lower than the reported first decomposition step temperature of $Ca(BH_4)_2$, T_{dec} = 367.[10] The second decomposition step at T = 450 °C is not observed in this study. However, a small shoulder is present at T = 379 °C assisted by a small hump in the H_2 MS signal (m/z = 2) which may indicate a second decomposition step. Indeed, the temperature is even further lowered in the second decomposition step (~ 70 °C) compared to the first step.

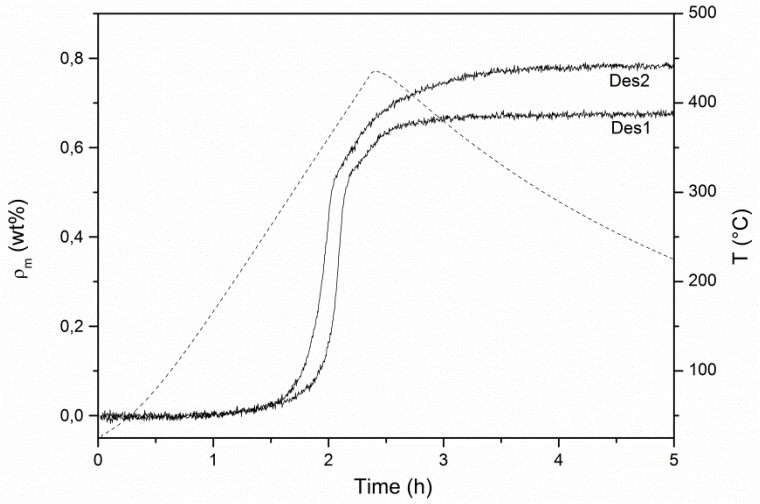

Figure S5. Sieverts measurement of the sample Ca_100bar_12h heated from RT to 450 °C with $\Delta T/\Delta t$ = 3 K/min.

The Sieverts' measurement is in good agreement with the observations in TG-DSC-MS. The gas release is initiated at T ~ 330 °C in the first desorption and at T ~ 310 °C in the second desorption whilst the gas release amounts to 0.68 and 0.79 wt%, respectively. This may indicate an activation of the compound during the first desorption.

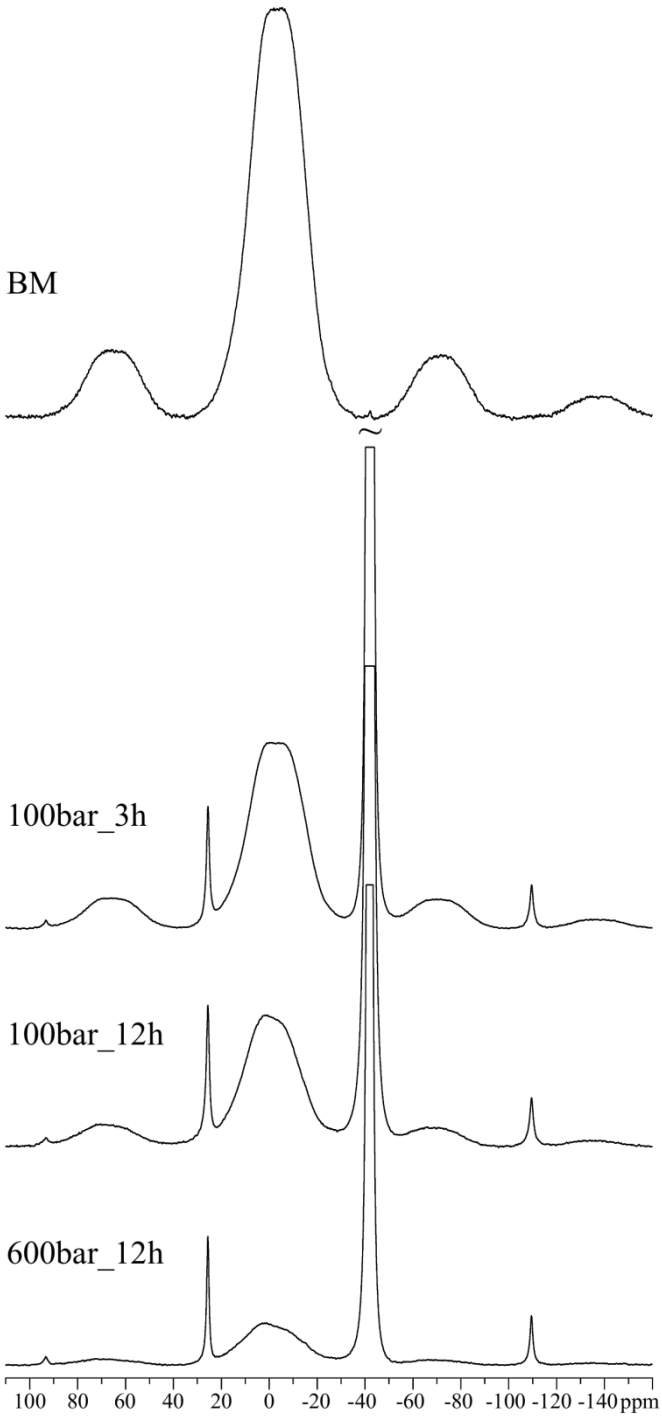

Figure S6. ^{11}B MAS NMR spectra (14.1 T, ν_R = 13.0 kHz) of the ball-milled AlB_2-NaH (BM) and and the Na_100bar_3h, Na_100bar_12h and Na_600bar_12h samples. The centerband from $NaBH_4$ is cut-off at approx. 1/12 of its total height in the spectra of the hydrogenated samples.

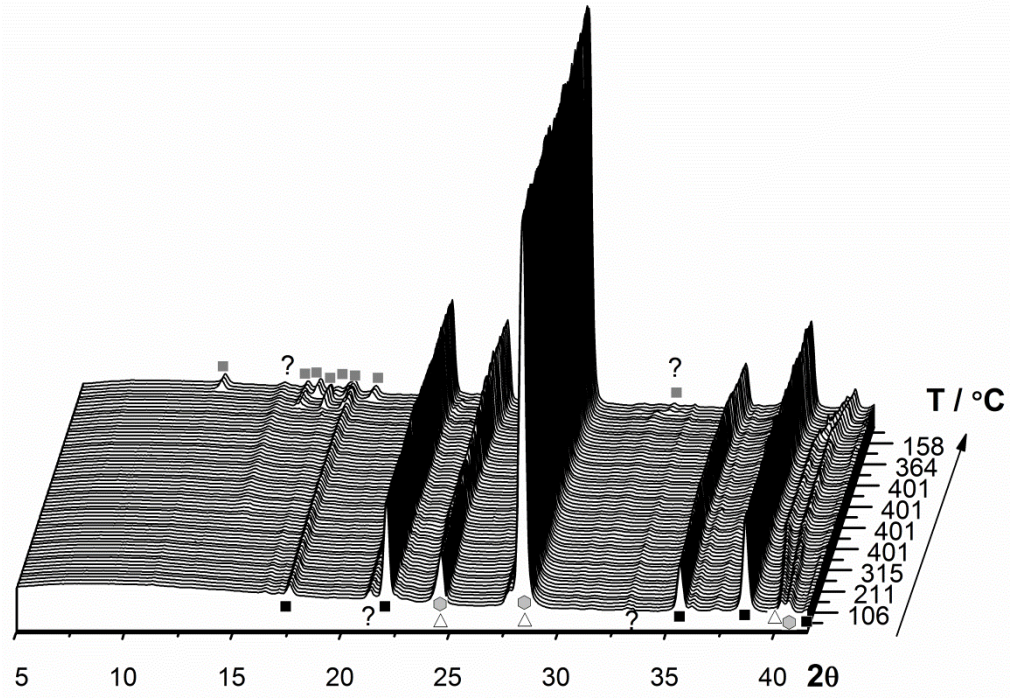

Figure S7. *In situ* SR-PXD data of LiH–AlB_2 (2:1) measured from RT to 400 °C ($\Delta T/\Delta t$ = 5 °C min^{-1}) and kept isothermal at T = 400 °C for 1 hour before cooling to RT ($\Delta T/\Delta t$ = 10 °C min^{-1}) ($p(H_2)$ = 100 bar, λ = 0.9938 Å). Symbols: grey square: $LiBH_4$, white triangle: LiH, black square: AlB_2, grey hexagon: Al, ?: unknown.

No changes in the powder pattern are observed during heating of the sample LiH–AlB_2 (2:1). At the isothermal step, T = 400 °C, $LiBH_4$ is expected to form in a molten state, and hence it is not observed in the X-ray diffractogram. However, an unidentified Bragg reflection appear at 2θ = 14.3° shortly after initiating the isothermal period, which is not correlated with any other change in the diffractogram. $LiBH_4$ is crystallizing during cooldown first into the high-temperature polymorph *h*-$LiBH_4$ at T ~ 224 °C before a phase transition into the low-temperature *o*-$LiBH_4$ at T ~ 84 °C.

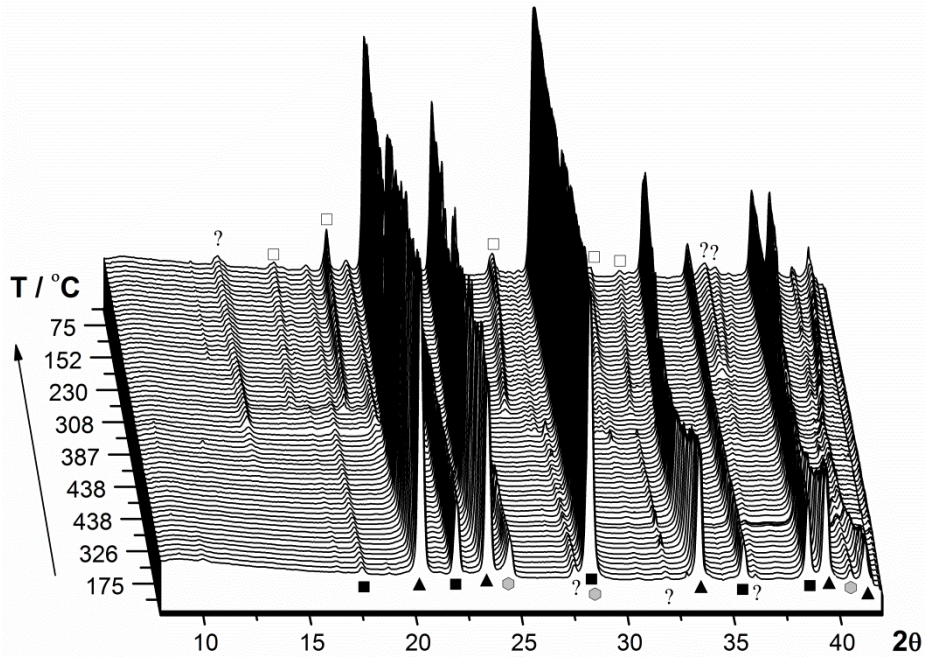

Figure S8. *In situ* SR-PXD data of NaH–AlB_2 (2:1) measured from RT to 440 °C ($\Delta T/\Delta t$ = 5 °C min^{-1}) and kept isothermal at T = 440 °C for 1 hour before cooling to RT ($\Delta T/\Delta t$ = 10 °C min^{-1}) ($p(H_2)$ = 100 bar, λ = 0.9938 Å). Symbols: white square: $NaBH_4$, black triangle: NaH, black square: AlB_2, grey hexagon: Al, ?: unknown.

During heating of the sample NaH–AlB_2 (2:1), no changes in the diffraction pattern are observed. Intensity of the Bragg reflections vary, however, the variation is correlated in all reflections and is assigned to instability of the radiation flux at the synchrotron. Initially, three unidentified Bragg reflections are present at 2θ = 27.5°, 31.9° and 36.1° which disappear slowly during the isothermal period. Similar to the LiH–AlB_2 (2:1) system, an unidentified Bragg reflection appear during the isothermal condition at 2θ = 13.3° which increase in intensity during cooldown. The sample is heated to above the melting point of $NaBH_4$. Hence, $NaBH_4$ begins to crystallize during cooldown at T ~ 385 °C and increase in intensity until reaching RT. At T ~ 300 °C yet two more unidentified Bragg reflections appear at 2θ = 36.1° and 36.4°. However, they do not seem to be correlated with other Bragg reflections.

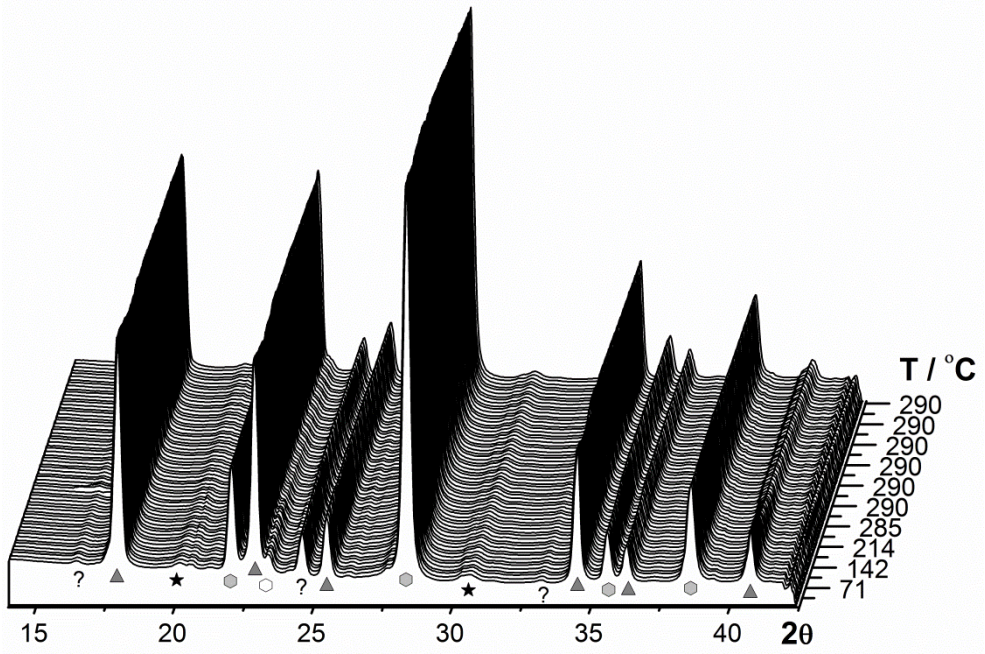

Figure S9. *In situ* SR-PXD data of MgH_2–AlB_2 (1:1) measured from RT to 290 °C ($\Delta T/\Delta t$ = 5 °C min^{-1}) ($p(H_2)$ = 100 bar, λ = 0.9938 Å). Symbols: grey triangle: MgH_2, white hexagon: Mg, black square: AlB_2, grey hexagon: Al, black star: WC.

During the measurement, no changes in the diffraction pattern are observed. Hence, no evidence of $Mg(BH_4)_2$ is found.

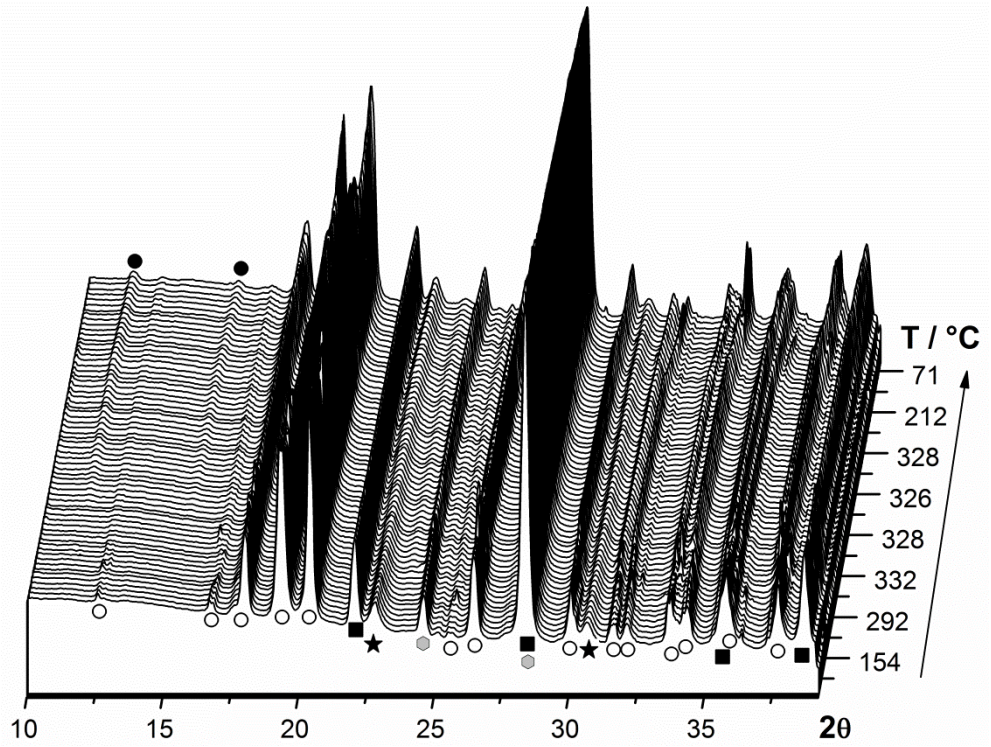

Figure S10. *In situ* SR-PXD data of CaH_2–AlB_2 (1:1) measured from RT to 350 °C ($\Delta T/\Delta t$ = 10 °C min^{-1}) and kept isothermal at T = 350 °C for 1 hour before cooling to RT ($\Delta T/\Delta t$ = 10 °C min^{-1}) ($p(H_2)$ = 100 bar, λ = 0.9938 Å). Symbols: white circle: CaH_2, black circle: β-$Ca(BH_4)_2$, black square: AlB_2, grey hexagon: Al, black star: WC.

Bragg reflections from β-$Ca(BH_4)_2$ starts to appear during the isothermal period and increase in intensity during cooldown. However, the Bragg reflections are weak in intensity indicating that not much is formed, probably due to slow kinetics. No phase transformation to α-$Ca(BH_4)_2$ is observed.

Table S1. Calculations on hydrogen capacity improvements if the AlB_2-MH_x (M = Li, Na, Ca) was implemented in a hydrogen fuel tank. The internal gas tank volume is 122.4 L and the powder filling level is set to either 25, 50 or 75 % of the tank volume.

		700 bar system		**350 bar system**	
		$\rho(H_2)$	39.24 kg/m^3 [11]	$\rho(H_2)$	23.33 kg/m^3 [11]
		$m(H_2)$	4.80 kg	$m(H_2)$	2.86 kg
System	m_{powder} **[kg]**	$m_{tot}(H_2)$ **[kg]**	**Increase in H_2 content (%)**	$m_{tot}(H_2)$ **[kg]**	**Increase in H_2 content (%)**
Filling level: 25%					
$2LiBH_4 + Al \leftrightarrow AlB_2 + 2LiH + 3H_2$	28.70	6.06	126.24	4.60	161.19
$2NaBH_4 + Al \leftrightarrow AlB_2 + 2NaH + 3H_2$	39.24	5.91	123.14	4.45	155.98
$Mg(BH_4)_2 + Al \leftrightarrow AlB_2 + MgH_2 + 3H_2$	31.39	5.95	123.82	4.49	157.13
$Ca(BH_4)_2 + Al \leftrightarrow AlB_2 + CaH_2 + 3H_2$	40.01	6.10	127.08	4.64	162.61
Filling level: 50%					
$2LiBH_4 + Al \leftrightarrow AlB_2 + 2LiH + 3H_2$	57.41	7.32	152.48	6.35	222.38
$2NaBH_4 + Al \leftrightarrow AlB_2 + 2NaH + 3H_2$	78.48	7.03	146.28	6.05	211.96
$Mg(BH_4)_2 + Al \leftrightarrow AlB_2 + MgH_2 + 3H_2$	62.78	7.09	147.64	6.12	214.25
$Ca(BH_4)_2 + Al \leftrightarrow AlB_2 + CaH_2 + 3H_2$	80.02	7.40	154.16	6.43	225.21
Filling level: 75%					
$2LiBH_4 + Al \leftrightarrow AlB_2 + 2LiH + 3H_2$	86.11	8.58	178.71	8.10	283.57
$2NaBH_4 + Al \leftrightarrow AlB_2 + 2NaH + 3H_2$	117.72	8.14	169.42	7.65	267.94
$Mg(BH_4)_2 + Al \leftrightarrow AlB_2 + MgH_2 + 3H_2$	94.18	8.24	171.47	7.75	271.38
$Ca(BH_4)_2 + Al \leftrightarrow AlB_2 + CaH_2 + 3H_2$	120.03	8.70	181.24	8.22	287.82

References

1 J.-P. Soulié, G. Renaudin, R. Černý and K. Yvon, *J. Alloys Compd.*, 2002, **346**, 200–205.
2 S. Gomes, H. Hagemann and K. Yvon, *J. Alloys Compd.*, 2002, **346**, 206–210.
3 H. I. Schlesinger and H. C. Brown, *J. Am. Chem. Soc.*, 1940, **62**, 3429–3435.
4 S. Orimo, Y. Nakamori, G. Kitahara, K. Miwa, N. Ohba, S. Towata and A. Züttel, *J. Alloys Compd.*, 2005, **404–406**, 427–430.
5 A. Züttel, P. Wenger, S. Rentsch, P. Sudan, P. Mauron and C. Emmenegger, *J. Power Sources*, 2003, **118**, 1–7.
6 P. Martelli, R. Caputo, A. Remhof, P. Mauron, A. Borgschulte and A. Züttel, *J. Phys. Chem. C*, 2010, **114**, 7173–7177.
7 G. Barkhordarian, T. R. Jensen, S. Doppiu, U. Bosenberg, A. Borgschulte, R. Gremaud, Y. Cerenius, M. Dornheim, T. Klassen and R. Bormann, *J. Phys. Chem. C*, 2008, **112**, 2743–2749.
8 Y. Filinchuk, E. Rönnebro and D. Chandra, *Acta Mater.*, 2009, **57**, 732–738.
9 M. Fichtner, K. Chlopek, M. Longhini and H. Hagemann, *J. Phys. Chem. C*, 2008, **112**, 11575–11579.
10 M. Aoki, K. Miwa, T. Noritake, N. Ohba, M. Matsumoto, H.-W. Li, Y. Nakamori, S. Towata and S. Orimo, *Appl. Phys. A*, 2008, **92**, 601–605.
11 E. W. Lemmon, M. L. Huber and M. O. McLinden, 2013.